Apr. 02, 2000

TESTING INTERMITTENCY OF THE GALACTIC STAR FORMATION HISTORY ALONG WITH THE INFALL MODEL

Tsutomu T. Takeuchi[1] **and Hiroyuki Hirashita**[1]

Department of Astronomy, Faculty of Science, Kyoto University, Sakyo-ku, Kyoto 606-8502, Japan

E-mail: takeuchi, hirasita@kusastro.kyoto-u.ac.jp

ABSTRACT

We analyze the star formation history (SFH) of the Galactic disk by using an infall model. Based on the observed SFH of the Galactic disk, we first determine the timescales of the gas infall into the Galactic disk ($t_{\rm in}$) and that of the gas consumption to form stars ($t_{\rm sf}$). Since each of the two timescales does not prove to be determined independently from the SFH, we first fix $t_{\rm sf}$. Then, $t_{\rm in}$ is determined so that we minimize χ^2. Consequently, we choose three parameter sets: ($t_{\rm sf}$ [Gyr], $t_{\rm in}$ [Gyr]) = (6.0, 23), (11, 12), and (15, 9.0), where we set the Galactic age as 15 Gyr. All of the three cases predict almost identical star formation history. Next, we test the intermittency (or variability) of the star formation rate (SFR) along with the smooth SFH suggested from the infall model. The large value of the χ^2 statistic supports the violent time-variation of the SFH. If we interpret the observed SFH with smooth and variable components, the amplitude of the variable component is comparable to the smooth component. Thus, intermittent SFH of the Galactic disk is strongly suggested. We also examined the metallicity distribution of G-dwarfs. We found that the true parameter set lies between ($t_{\rm sf}$ [Gyr], $t_{\rm in}$ [Gyr]) = (6, 23) and (11, 12), though we should need a more sophisticated model including the process of metal enrichment within the Galactic halo.

Subject headings: Galaxy: evolution — Galaxy: stellar content — methods: statistical — stars: abundances — stars: formation

1. INTRODUCTION

In the field of the Galactic chemical evolution, Eggen, Lynden-Bell, & Sandage (1962) have inspired the modeling. From the correlation between the ultraviolet excess and orbital eccentricity

[1]Research Fellows of the Japan Society for the Promotion of Science.

of stars, they concluded that the Galaxy formed by collapse on a free-fall timescale from a single protogalactic cloud. An alternative picture of halo formation is proposed by Searle & Zinn (1978). They argued that Galactic system is formed from the capture of fragments such as dwarf galaxies over a longer timescale than that proposed by Eggen et al. In any case, determining the timescale of the infall of matter and the chemical enrichment is an important problem to resolve the formation mechanism of the Galactic system. Indeed, there have been a number of papers that investigated the formation and chemical evolution of the Galaxy (e.g., Matteucci & François 1989) and spiral galaxies (e.g., Lynden-Bell 1975; Sommer-Larsen 1996).

Many models of the star formation history (SFH) of the Galaxy includes the formation of the Galactic disk by gas infall. This scenario (so-called the infall model) is consistent with the age-metallicity relation of the disk stars (e.g., Twarog 1980), if a reasonable SFH is applied. Moreover, the infall model provides a physically reasonable way of solving the G-dwarf problem (e.g., Pagel 1997, p.236), contrary to the closed-box model which tends to overpredict the number of the low-metallicity stars.

One of the factors that determine the star formation rate (SFR) is the gas content of galaxies. Indeed, the SFR and the gas density is closely related to each other (Kennicutt 1998), and this relation is generally called the Schmidt law (Schmidt 1959). The SFR and the gas density, ρ, are related as SFR $\propto \rho^n$, where $n = 1 - 2$. In the one-zone model, the relation is simply assumed to be described with SFR $\propto M_{\rm g}^n$, where $M_{\rm g}$ is the gas mass in the galaxy.

Though the "classical" infall model is widely accepted, there are observational data that suggest the intermittent star formation activities in spiral galaxies. Kennicutt, Tamblyn, & Congdon (1994) showed the ratio of present-to-past SFR in spiral sample has a significant scatter. More recently, Tomita, Tomita & Saitō (1996) analyzed the far-infrared to B-band flux ratio $f_{\rm FIR}/f_B$ of 1681 spiral galaxies (see also Devereux & Hameed 1997). The indicator $f_{\rm FIR}/f_B$ also represents the ratio between the present SFR and the averaged SFR during the recent Gyr. They showed the order-of-magnitude spread of $f_{\rm FIR}/f_B$ and suggested the violent temporal variation of the SFR.

The intermittency of the SFH in the Galactic disk is recently suggested by Rocha-Pinto et al. (2000; hereafter R00). They derived the SFH of the Galactic disk from observed age distribution of the late-type stars and suggested that the star formation activity of the disk is intermittent or violently variable. They tested to show that the variation is of statistical significance. Their test are based on the null hypothesis that the SFR of the Galaxy is temporally "constant", but their derived SFH indicates that the SFR around 10–15 Gyr ago is significantly smaller than that around 0–10 Gyr ago. This trend of the Galactic SFR can be interpreted along with the infall scenario of the Galactic disk formation: Gas-infall to the Galactic disk occurred in the first ~ 5 Gyr. Thus it is an important work to interpret their data through the infall model and to examine whether the variation of SFR is still significant even in the infall scenario.

In this paper, we re-analyze the data by R00 in the context of the infall model. In the next section, we briefly review the derivation of the SFH in the Galactic disk by R00. Next, in §3, we present the formulation of the infall model, based on which we test the data by R00 statistically. In §4, we interpret the observed SFH by two components; underlying infall-model component and violently variable component. In the same section, possible physical mechanisms for the variation of star formation are also presented. Finally, we summarize the content in §5.

2. THE DATA

R00 provided the SFH of the Galaxy inferred from the stellar age of the solar neighborhood. They used 552 late-type stars. The age of each star is estimated from the chromospheric emission in the Ca II H and K lines (Soderblom, Duncan, & Johnson 1991). After metallicity-dependent age correction, completeness correction, and scale-height correction[2], they derived the age distribution of the stars. Then, after correcting the stars that is not alive at present, they derived the SFH of the Galactic disk in their Figure 2. The discussion in this paper is based on Figure 2 of R00.

R00 concluded that the inferred SFH is representative of the SFH of the whole disk, since the timescale of the diffusion of stars to the kpc scale is ~ 0.2 Gyr, which is much shorter than the Galactic age. Thus, in the next section, we model the Galactic SFH by a one-zone model to extract the *global* property of the SFH. The difference between the one-zone and the multi-zone treatment is seen in Figure 6 of Sommer-Larsen (1996), where we see that the one-zone treatment is a good approximation.

3. SFH FROM INFALL MODEL

In this section, we give a physical interpretation of the SFH by R00. First, we adopt the infall model for the interpretation, since the model has been successful in reproducing the age-metallicity relation of stars in the solar neighborhood (e.g., Pagel 1997). Next, we infer the timescales of the following two processes; the infall of gas into the Galactic disk and the gas consumption to form stars. Finally, we examine whether the intermittent SFH proposed in R00 is of statistical significance.

3.1. Model Description

We assume the one-zone model: The gas mass in the Galaxy is treated as a function of time, $M_{\rm g}(t)$. The time evolution of the gas mass is determined by the infall from the halo, whose rate is described by $F(t)$, the consumption by star formation, $\psi(t)$, and the recycling from stellar mass loss. If the instantaneous recycling approximation is adopted (Tinsley 1980), the time evolution of

[2]The scale height is dependent on the age of stars.

the gas mass in the Galaxy is described by

$$\frac{\mathrm{d}M_{\mathrm{g}}}{\mathrm{d}\,t} = -(1-R)\psi + F \ , \tag{1}$$

where R is the returned fraction from stellar mass loss, described by

$$R = \int_{m_t}^{m_u} (m - w_m)\phi(m)\,\mathrm{d}m \ . \tag{2}$$

Here, $\phi(m)$ is the initial mass function (IMF) of stars, m_t is the present turnoff mass ($1M_\odot$), m_u is the upper cutoff of the stellar mass ($100M_\odot$), and w_m is the remnant mass (we assume $w_m = 0.7M_\odot$ for $m < 4M_\odot$ and $w_m = 1.4M_\odot$ for $m > 4M_\odot$). The IMF is normalized so that the integral of $m\phi(m)$ in the full range of the stellar mass becomes unity. When the Salpeter IMF, $\phi(m) \propto m^{-2.35}$ (Salpeter 1955) with the lower cutoff of $0.1\,M_\odot$ and the upper cutoff of $100\,M_\odot$ is assumed, $R = 0.32$. Pagel (1997) derived a similar value for R by using a different form of IMF and remnant mass ($R = 0.2 - 0.3$), and commented that the uncertainty in R is ~ 0.1.

Since the normalization of the SFR and statistical test become much more complicated unless the SFR is presented by analytic function, we adopt the instantaneous recycling approximation for clarity in this section. The analytic form makes it significantly easy to perform the statistical test in §3.3. We examine the propriety of adopting the instantaneous recycling approximation to this problem in §4.2.

In this paper, the timescale of the gas infall onto the Galactic disk, t_{in}, will be determined by a fitting to the observational data in §3.3. For the convenience of the fitting, we assume the infall rate is expressed by an analytic function. A natural form is the following exponential function (Pagel 1997, p.242):

$$F(t) = \frac{M_0}{t_{\mathrm{in}}}\exp(-t/t_{\mathrm{in}}), \tag{3}$$

where M_0 indicates the total mass that can fall into disk; in other words,

$$\int_0^\infty F(t)\,\mathrm{d}t = M_0. \tag{4}$$

Normalizing the equation (1) by M_0 leads

$$\frac{\mathrm{d}f_{\mathrm{g}}}{\mathrm{d}\,t} = -(1-R)\frac{f_{\mathrm{g}}}{t_{\mathrm{sf}}} + \frac{1}{t_{\mathrm{in}}}\exp\left(-t/t_{\mathrm{in}}\right) \ , \tag{5}$$

where

$$f_{\mathrm{g}} \equiv \frac{M_{\mathrm{g}}}{M_0} \ . \tag{6}$$

The Schmidt law of $n = 1$ (§1) is assumed as follows:

$$\tilde{\psi} \equiv \psi/M_0 = f_{\mathrm{g}}/t_{\mathrm{sf}} \ , \tag{7}$$

where $t_{\rm sf}$ indicates the timescale for the gas to be converted to stars (i.e., the gas consumption timescale). Then, we can express the solution of equation (5) analytically as

$$f_{\rm g}(t) = \frac{\beta}{1-\beta}\left(e^{-t/t_{\rm in}} - e^{-(1-R)t/t_{\rm sf}}\right) , \quad (8)$$

$$\beta \equiv \frac{t_{\rm sf}}{(1-R)t_{\rm in}} . \quad (9)$$

One of the goals in this paper is to infer the two timescales, $t_{\rm in}$ and $t_{\rm sf}$ from the SFH in R00. Thus, we define the SFR at the Galactic age of t, $\tilde{\psi}$, as

$$\tilde{\psi} = \tilde{\psi}(t\,;\,t_{\rm in}, t_{\rm sf}) \equiv f_{\rm g}/t_{\rm sf} . \quad (10)$$

For the following discussions it is convenient to define the averaged SFR for the normalization of ψ. The averaged SFR, $\langle\tilde{\psi}\rangle$, is defined by

$$\langle\tilde{\psi}\rangle \equiv \frac{1}{T_{\rm G}}\int_0^{T_{\rm G}} \tilde{\psi}\,{\rm d}t. \quad (11)$$

Equations (8) and (10) lead the averaged SFR as

$$\langle\tilde{\psi}\rangle = \frac{1}{T_{\rm G}}\int_0^{T_{\rm G}} \frac{\beta}{(1-\beta)t_{\rm sf}}\left(e^{-t/t_{\rm in}} - e^{-(1-R)t/t_{\rm sf}}\right){\rm d}t, \quad (12)$$

where $T_{\rm G}$ is the age of the Galactic disk and we take $T_{\rm G} = 15$ Gyr following R00. Then we obtain

$$\frac{\tilde{\psi}}{\langle\tilde{\psi}\rangle} = \frac{e^{-\tau/\tau_{\rm in}} - e^{-(1-R)\tau/\tau_{\rm sf}}}{\tau_{\rm in}\left(1-e^{-1/\tau_{\rm in}}\right) - \dfrac{\tau_{\rm sf}}{(1-R)}\left(1-e^{-(1-R)/\tau_{\rm sf}}\right)} \equiv \Psi(\tau\,;\,\tau_{\rm in}, \tau_{\rm sf}) , \quad (13)$$

where $\tau \equiv t/T_{\rm G}$, $\tau_{\rm in} \equiv t_{\rm in}/T_{\rm G}$, and $\tau_{\rm sf} \equiv t_{\rm sf}/T_{\rm G}$. Here we note that

$$\int_0^1 \Psi(\tau)\,{\rm d}\tau = 1 . \quad (14)$$

3.2. Trend Estimation

We extract the overall "trend" from the data of R00. We used the smoothing method developed in the field of the exploratory data analysis (EDA), as well as the ordinary moving average. The EDA smoothing is based on the moving median, which is is known to be quite robust against outliers in the datasets compared with the moving average (e.g., Hoaglin, Mosteller, & Tukey 1983). Since the SFH in R00 violently varies with time, the EDA procedure is expected to be suitable for the problem. Detailed procedures are summarized in the appendix. The smoothed results with the above two procedures are shown in Figure 1. The original data are depicted by the dotted histogram. In the upper panel, we show the smoothing results by moving average. Details of the moving average method is extensively discussed in e.g., Hart (1997). The dot-dot-dot-dashed line is the smoothed SFR with smoothing kernel width of 1.2 Gyr, strong dashed line is the smoothed SFR with 2.0 Gyr kernel, and dot-dashed line is the smoothed SFR with 2.8 Gyr kernel. In the lower panel, the dashed line represents the moving average of 2.0 Gyr kernel, and the solid line is the EDA smoothed SFH. We observe that the 1.2-Gyr kernel is not sufficient to smooth the varying SFH. This means that the timescale of the variation is less than ~ 2 Gyr. Possible mechanisms of the variation that works in less than 2 Gyr are listed in §4.4.

We see that the two results yield consistent trends, but the EDA result is not affected by the sudden jump of the values compared with the moving average as clearly seen at $T_{\rm G} - t = 10 - 15$ Gyr. We find the rise of the SFR in the early epoch. This is interpreted as being the gradual increase of gas by the infall. Thus we suggest that the overall SFH of the Galaxy is well described by the infall scenario. We statistically infer the infall timescale and the gas consumption timescale in the next section. We will also examine whether the 'residual' deviated from the trend is of statistical significance there.

3.3. Parameter Estimation and Statistical Test

In this subsection we perform a statistical test for the observed Galactic (normalized) SFR, $\Psi_{\rm obs}$ (shown as SFR/$\langle$SFR$\rangle$ in R00) with respect to that inferred from the infall model. The observed data are binned as $\Psi_{{\rm obs}i}$, $i = 1, 2, \ldots, k$. Once the parameter set ($\tau_{\rm in}$, $\tau_{\rm sf}$) is fixed, we can estimate these parameters from the modified Pearson's chi-square statistic, ${\chi_0}^2$ (see e.g., Rao 1973, p.352):

$$ {\chi_0}^2 \equiv \sum_{i=1}^{k} \frac{(n_i - N\Psi_i^{\rm int})^2}{n_i} = N \sum_{i=1}^{k} \frac{(\Psi_{{\rm obs},i}^{\rm raw} - \Psi_i^{\rm int})^2}{\Psi_{{\rm obs},i}^{\rm raw}} , \tag{15} $$

where n_i is the raw number of stars in the i-th bin, N is the sample size (in this case $N = 552$), $\Psi_{{\rm obs},i}^{\rm raw}$ is the raw normalized SFR without completeness corrections, and $\Psi_i^{\rm int}$ is the binned theoretical SFR which we would have observed under the same condition as $\Psi_{{\rm obs},i}^{\rm raw}$. However, since the SFR in Figure 2 of Rocha-Pinto et al. (2000a) is corrected for the selection biases when they have derived the value, we must include the effect of the incompleteness correction in the statistical analysis. We set $n_{{\rm cor},i} = c_i n_i$, then we obtain

$$ c_i = \frac{n_{{\rm cor},i}}{n_i} = \frac{N_{\rm cor}\Psi_{{\rm obs},i}^{\rm cor}}{N_{\rm raw}\Psi_{{\rm obs},i}^{\rm raw}} = \frac{\Psi_{{\rm obs},i}^{\rm cor}}{\Psi_{{\rm obs},i}^{\rm raw}} , \tag{16} $$

where $\Psi_{{\rm obs},i}^{\rm cor}$ is the corrected SFR as shown in R00. Here, we fix the data size as $N_{\rm cor} = N_{\rm raw} = N$. As long as $N_{\rm cor} \sim N_{\rm raw}$, the statistical significance is not affected by this procedure. Therefore we have the model value

$$ \Psi_i = c_i \Psi_i^{\rm int} , \tag{17} $$

where

$$\Psi_i \equiv \frac{1}{\tau_{i+1} - \tau_i} \int_{\tau_i}^{\tau_{i+1}} \Psi(\tau)\, \mathrm{d}\tau \ . \tag{18}$$

In addition, R00 note that the error bar is a Poisson fluctuation, thus the i-th error bar, σ_i, can be described as

$$\sigma_i = \frac{c_i}{N} \left(N \Psi_{\mathrm{obs},i}^{\mathrm{raw}} \right)^{1/2} = \left(\frac{c_i \Psi_{\mathrm{obs},i}^{\mathrm{cor}}}{N} \right)^{1/2} \ . \tag{19}$$

Considering the above, we observe

$$\begin{aligned} {\chi_0}^2 &= N \sum_{i=1}^{k} \frac{\left(\frac{\Psi_{\mathrm{obs},i}^{\mathrm{cor}}}{c_i} - \frac{\Psi_i}{c_i} \right)^2}{\frac{\Psi_{\mathrm{obs},i}^{\mathrm{cor}}}{c_i}} = N \sum_{i=1}^{k} \frac{(\Psi_{\mathrm{obs},i}^{\mathrm{cor}} - \Psi_i)^2}{c_i \Psi_{\mathrm{obs},i}^{\mathrm{cor}}} \\ &= \sum_{i=1}^{k} \frac{(\Psi_{\mathrm{obs},i}^{\mathrm{cor}} - \Psi_i)^2}{{\sigma_i}^2} \ . \end{aligned} \tag{20}$$

For the numerical convenience, we fix $\Psi_{\mathrm{obs},i}^{\mathrm{cor}} = \Psi_i = 0$ at $\tau = 0$, and the other 37 points are used for the inference (i.e., $k = 37$).

As we will see later, τ_{sf} and τ_{in} are not determined independently. Thus, we will fix one of the parameters. Since τ_{sf} is extensively investigated by Kennicutt et al. (1994), we first fix τ_{sf}. Then, τ_{in} is determined by minimizing ${\chi_0}^2$. As representative values for the gas consumption timescale, τ_{sf}, we choose 0.4, 0.7 and 1.0 ($t_{\mathrm{sf}} = 6.0$, 11, and 15 Gyr, respectively)[3]. The best-fit τ_{in} and ${\chi_0}^2$ for each τ_{sf} are listed in Table 1. The best-fit τ_{in}'s are 1.5, 0.8, 0.6, respectively, and ${\chi_0}^2 = 172$. The three cases are presented in Figure 2. We see that the three parameter sets describes an almost identical SFH. This means that the two parameters, τ_{sf} and τ_{in} are strongly correlated and it is almost impossible to determine τ_{sf} and τ_{in} independently.

We are able to test the goodness of fit between Ψ_{obs} and Ψ_i at the same time by evaluating ${\chi_0}^2$ with respect to the χ^2-statistics with $(k-2)$ degrees of freedom. If ${\chi_0}^2 > \chi^2(k-2, \alpha)$, then the hypothesis that the observed SFH is produced by the infall scenario is rejected with confidence level $(1-\alpha)$. In fact, even if we set $\alpha = 0.01$, $\chi^2(k-2, \alpha) = 60$. Thus, we conclude that the data of R00 is not produced by the "classical" infall model. This clearly indicates the fact that the Galactic SFH is not continuous, but strongly intermittent or variable.

[3]If we set $\tau_{\mathrm{sf}} < 0.4$, we obtain an unreasonably large $\tau_{\mathrm{in}} (\gtrsim 2)$ for the best fit parameter.

4. DISCUSSIONS

4.1. Metallicity and G-dwarf Problem

One of the prime motivation for infall models is that they provide a physically reasonable way of solving the G-dwarf problem (Pagel 1997 and references therein). Thus, in this section, we examine the chemical evolution of the Galaxy.

Under the one-zone treatment and the instantaneous recycling approximation, the time evolution of the abundance of the heavy element, whose species is labeled by i ($i =$ O, C, Si, Mg, Fe, ...), is expressed as

$$\frac{\mathrm{d}M_i}{\mathrm{d}t} = -X_i\psi + E_i + X_i^{\mathrm{f}}F(t), \tag{21}$$

where M_i, X_i, E_i and X_i^{f} are the total mass of heavy element i, the abundance of i (i.e., $X_i \equiv M_i/M_{\mathrm{g}}$), the total injection rate of element i from stars, and the abundance of the infalling gas, respectively (Tinsley 1980). Here, E_i is expressed as

$$E_i = (RX_i + Y_i)\psi, \tag{22}$$

where R is defined in equation (2) and Y_i is the mass fraction of the element i newly produced and ejected by stars; in other words,

$$Y_i = \int_{m_t}^{m_u} mp_i(m)\phi(m)\,\mathrm{d}m, \tag{23}$$

where $p_i(m)$ is the fraction of mass converted into the element i in a star of mass m. Adopting the Salpeter's IMF and the stellar yield by Maeder (1992), $Y_{\mathrm{O}} = 1.8\times 10^{-2}$, where we adopt the oxygen as a tracer of heavy elements (i.e., $i =$ O; Lisenfeld & Ferrara 1998; Hirashita 1999). Combining equations (1), (3), (7), (21), and (22), we obtain

$$f_{\mathrm{g}}\frac{\mathrm{d}X_i}{\mathrm{d}\tau} = \frac{f_{\mathrm{g}}Y_i}{\tau_{\mathrm{sf}}} - \frac{X_i - X_i^{\mathrm{f}}}{\tau_{\mathrm{in}}}e^{-\tau/\tau_{\mathrm{in}}}. \tag{24}$$

Since the time-evolution of f_{g} is solved in equation (8), equation (24) can be integrated to obtain X_i as a function of $\tau(= t/T_{\mathrm{G}})$. We hereafter choose oxygen as a tracer of the metallicity; i.e., $i =$ O and assume $X_{\mathrm{O}}^{\mathrm{f}} = 0.01X_{\mathrm{O},\odot}$. For a more detailed modeling, we should include the metal enrichment within the Galactic halo (e.g., Ikuta & Arimoto 1999).

The result is shown in Figure 3 for the three parameter sets in Table 1, where $X_{\mathrm{O},\odot} = 0.013$ represents the solar oxygen abundance (Whittet 1992, p.42). The solid, dashed, and dash-dotted lines present the cases of $(\tau_{\mathrm{sf}},\, \tau_{\mathrm{in}}) = (0.4, 1.5), (0.7, 0.8)$, and $(1.0, 0.6)$, respectively. We also present the observational data of age-metallicity relation by Rocha-Pinto et al. (2000b) (see their Table 3), where we assume that $0.7\,[\mathrm{Fe/H}] = [\mathrm{O/H}] \equiv \log(X_{\mathrm{O}}/X_{\mathrm{O},\odot})$ by using Edvardsson et al. (1993). The true parameter set which reproduce the observational data points seems to lie between the solid line $(\tau_{\rm sf},\, \tau_{\rm in}) = (0.4, 1.5)$ and $(\tau_{\rm sf},\, \tau_{\rm in}) = (0.7, 0.8)$, though the discrepancy at the lower-metallicity side is prominent. But if the infalling gas is more enriched than have been assumed, this discrepancy might be resolved. We should also note the large scatter of the relation (Fig. 13 of Rocha-Pinto et al. 2000b) and the uncertainty in the above relation between [Fe/H] and [O/H].

The infall timescale is larger than that in Sommer-Larsen & Antonuccio-Delogu (1993), who gave 3.4 Gyr. The difference comes not only from the different way of modeling but also from the no prominent decline of the recent SFR as presented in Figure 2.

The G-dwarf problem is also tested along with our model. The probability distribution function $P(\log X_{\rm O})$ of the metallicity is calculated from our model as

$$P(\log X_{\rm O})\, {\rm d}\log X_{\rm O} = \Psi\, {\rm d}\tau. \tag{25}$$

Using equations (24) and (25), we obtain the following analytical expression for P:

$$P(\log X_{\rm O}) = (\ln 10)\ \Psi(\tau) X_{\rm O}(\tau) \left[\frac{Y_{\rm O}}{\tau_{\rm sf}} - \frac{X_{\rm O}(\tau) - X_{\rm O}^{\rm f}}{\tau_{\rm in} f_{\rm g}(\tau)} e^{-\tau/\tau_{\rm in}}\right]^{-1}, \tag{26}$$

where τ is a function of $X_{\rm O}$ and the functional form is determined by solving equation (24). In comparing the distribution function with the observational data, we should take into account the scatter of the data. Here, we simply convolve P with a Gaussian kernel as

$$P_{\rm conv}(\log X_{\rm O}) \equiv \int_{-\infty}^{\infty} P(u)\, \frac{1}{\sqrt{2\pi}\,\sigma}\, \exp\left[-\frac{(\log X_{\rm O} - u)^2}{2\sigma^2}\right] {\rm d}u, \tag{27}$$

where we adopt $\sigma = 0.1$ to compare with Rocha-Pinto & Maciel (1996). We adopt these data because we would like to use a sample of G-dwarfs, whose lifetime is as long as the age of the universe. The result is shown in Figure 4. The solid, dashed, and dash-dotted lines present the cases of $(\tau_{\rm sf},\, \tau_{\rm in}) = (0.4, 1.5), (0.7, 0.8)$, and $(1.0, 0.6)$, respectively. The histogram shows the data by Rocha-Pinto & Maciel (1996), where $0.7\,[{\rm Fe/H}] = [{\rm O/H}]$ is assumed and the integrated number is normalized to unity. We see the same trend as Figure 3: Again we see that the true parameters lie between the solid line and the dashed line. As mentioned above, we should include the detailed enrichment process within the Galactic halo as e.g., in Ikuta & Arimoto (1999). However, since the aim of this paper is to examine the intermittent SFH proposed by R00, we do not examine the chemical evolution further.

4.2. Comment on the Instantaneous Recycling Treatment

The instantaneous recycling approximation is adopted only because it provides a very convenient way to obtain an analytic SFH, which is easily applied to the statistical analysis in §3.3. However, if we fix $t_{\rm sf}$, the instantaneous recycling treatment tends to overestimate the rate of gas consumption to form stars due to the instantaneously recycled gas, which should be recycled with a delay in the realistic situation. Thus, we here examine the effect of the delayed recycling. We examine the opposite extreme case where the effect of the delayed recycling is significant: The gas is never recycled. In other words, we examine the case of $R = 0$.

In Figure 5, we present the result for $R = 0$ for the three parameters $(\tau_{\rm sf},\, \tau_{\rm in}) = (0.4,\, 1.5)$, $(0.7,\, 0.8)$, and $(1.0,\, 0.6)$ with the thick lines. The thin lines represent the case where $R = 0.32$; i.e., the same as Figure 3. We adopt the same normalization for both sets of lines (equation 14). Comparing the thick and thin lines, we see the more decline of the SFR in the recent epoch in the non-recycling case than the thin lines. This is because the gas consumption timescale is shorter in the non-recycling case (Kennicutt et al. 1994). However, we stress that the variation of the observed SFH (R00) is so large that the difference between the instantaneous and non-instantaneous treatments does not affect the conclusion that the SFR is violently variable.

4.3. Two-Component Model of the Star Formation Rate

Since the observed SFH cannot be reproduced by a simple infall model, we introduce a stochastically varying residual and modify the model as follows:

$$\Psi_{\rm obs}(\tau) = \Psi_{\rm infall}(\tau) + \varepsilon \ , \tag{28}$$

where $\Psi_{\rm infall}(t)$ is the estimated best-fit infall model in the above discussion, and the residual, ε, is produced by a probability distribution with zero mean and dispersion σ^2. We simply assume that σ^2 is time-independent. Since ε is estimated for each of the 37 bins, we can show a distribution of ε (Figure 6). The estimated sample dispersion $\sigma^2 = 0.22$ ($\sigma = 0.47$). Considering the uncertainty in the age estimation in R00, the time-variation of the SFR is blurred with the uncertainty, as commented in R00. Thus, the above value of σ can still be underestimated. Therefore, we conclude that the σ is at least comparable to (perhaps larger than) $\Psi_{\rm infall}$.

If we assume that the large variation of the SFR is typical of spiral galaxies, the star formation activities of them should show a variety. The large value of the variance (σ) is consistent with previous works that suggested the variety of star formation activities of spiral galaxies (Kennicutt et al. 1994; Tomita et al. 1996; Devereux & Hameed 1997). Furthermore, the kurtosis of the residual, $K = -0.81$, which means that ε is distributed flatly and is not strongly concentrated around the mean. Indeed, in the Figure 8 of Tomita et al. 1996, there seems to be little concentration of star formation activity around the mean, which is consistent with the flat distribution in Figure 6.

4.4. Possible Mechanisms for the Variation of SFH

Here, we consider what mechanisms are possible for the violent time-variation of SFR in the Galactic disk. We mention the following two mechanisms.

The first possibility is that the infall into the Galactic disk is a stochastic process. If an infalling gas is in the form of a cloud or a small-sized galaxy, such gas may induce a burst of star formation and increase SFR instantaneously. Indeed, infall of small galaxy seems to occur frequently seeing that the Sagittarius dwarf galaxy is now infalling to the Galaxy (Ibata, Gilmore, & Irwin 1994). The high-velocity clouds (Wakker & van Woerden 1997) may fall into the Galactic disk stochastically and induce stochastic bursts of star formation.

The second possibility is that the interstellar medium is a non-linear open system. A non-linear open system often shows a limit-cycle behavior of physical quantities (Nicolis & Prigogine 1977). The application of the non-linear-open-system model to the interstellar medium is described in Ikeuchi & Tomita (1983). According to their model, the fractional mass of the cold component ($X_{\rm c}$) can oscillatory change. Recently, Kamaya & Takeuchi (1997) suggested that the SFR varies oscillatory if the Schmidt law of SFR $\propto X_{\rm c}^2$ is assumed, where $X_{\rm c}$ is the mass ratio of the cold gas to the whole gas (see also Ikeuchi 1988 for a review and Hirashita & Kamaya 2000 for a recent development on this theme).

5. SUMMARY

In the context of the infall model, we re-analyzed the SFH of the Galaxy derived observationally by R00. We test to examine whether variation of the star formation rate proposed by R00 is significant.

We first statistically infer the timescales of the gas infall into the Galactic disk ($t_{\rm in}$) and that of the gas consumption to form stars ($t_{\rm sf}$). Since each of two timescales are not determined independently, we first fix $t_{\rm sf}$. Then, $t_{\rm in}$ is determined so that we minimize χ^2. Consequently, we choose three parameter sets: $(t_{\rm sf}\,[{\rm Gyr}],\, t_{\rm in}\,[{\rm Gyr}]) = (4.5, 33), (10.5, 9.0)$, and $(15, 7.5)$, where we set the Galactic age as 15 Gyr. All of the three cases predict an almost identical SFH. The parameter set that seems to fit best to the age-metallicity relation and the metallicity distribution of the G-dwarfs is $(t_{\rm sf}\,[{\rm Gyr}],\, t_{\rm in}\,[{\rm Gyr}]) = (10.5,\, 9.0)$. The infall timescale is larger than that in Sommer-Larsen & Antonuccio-Delogu (1993), who gave 3.4 Gyr. The difference comes not only from the different way of modeling but also from the no prominent decline of the recent SFR as presented in Figure 2.

Next, we test the intermittency (or violent variability) along with the smooth SFH suggested from the infall model. The large value of χ^2 statistic supports the violent variation of the SFH. Then, we interpret the observed SFH with the two components; underlying smooth component described by the infall model, and violently variable component. We find that the variation of the latter component is comparable to the former.

As a test of the models, we also examine the age-metallicity relation and the metallicity distribution of the Galactic stars. Consequently, we observe that the degeneracy of the three parameters are resolved and find that the true parameter set seems to lie between $(t_{\rm sf}\,[{\rm Gyr}],\, t_{\rm in}\,[{\rm Gyr}]) =$

(10.5, 9.0) and $(4.5, 33)$.

Finally, two physical mechanisms for the variable SFH are suggested. One is the stochastic infall of the clouds or small galaxies, and the other is the non-linear oscillation of the SFR due to the limit-cycle behavior of the fractional mass of the cold-gas component.

We first thank J. Sommer-Larsen, the referee, whose comments much improved the quality of this paper. We also thank H. Kamaya, A. Tomita, T. T. Ishii, S. Mineshige, and M. Saitō for useful discussions and kind helps. We are grateful to K. Yoshikawa for an excellent computational environment. This work is supported by the Research Fellowship of the Japan Society for the Promotion of Science for Young Scientists. We made extensive use of the NASA's Astrophysics Data System Abstract Service (ADS).

A. SMOOTHING WITH MOVING MEDIAN

In this appendix, we explain the details of the EDA smoothing based on the moving median. The procedure is as follows:

1. We take the moving median of three sequential values of the original data. For the boundary data, we use the median of the following:

$$\hat{x}_1 = \mathrm{median}(x_2 - 2(x_2 - x_3), x_1, x_2) \ , \tag{A1}$$

$$\hat{x}_n = \mathrm{median}(x_n + 2(x_{n-1} - x_{n-2}), x_{n-1}, x_n) \ , \tag{A2}$$

   where $\hat{x}_i$ is the smoothed value.

2. We perform the splitting of the plateau of the median-smoothed data sequence, i.e. when we find the same value $\hat{x}_i$ and $\hat{x}_{i+1}$, we substitute

$$\hat{\hat{x}}_i = \mathrm{median}(x_{i-1} + 2(x_{i-1} - x_{i-2}), x_i, x_{i-1}), \tag{A3}$$

$$\hat{\hat{x}}_{i+1} = \mathrm{median}(x_{i+2} - 2(x_{i+3} - x_{i+2}), x_{i+1}, x_{i+2}). \tag{A4}$$

   into $\hat{x}_i$ and $\hat{x}_{i+1}$, respectively.

3. We, then, take the mean of $\hat{x}_{i-1}$ and $\hat{x}_{i+1}$ (we denote them as $\tilde{x}_i$). Finally, we derive the mean of $\hat{x}_i$ and $\tilde{x}_i$.

This method is often used in the econometric and biometric researches, and provides successful results.

REFERENCES

Devereux, N. A., & Hameed, S. 1997, AJ, 113, 599

Edvardsson, B., Andersen, J., Gustafsson, B., Lambert, D. L., Nissen, P. E., & Tomkin, J. 1993, A&A, 275, 101

Eggen, O. J., Lynden-Bell, D., & Sandage, A. R. 1962, ApJ, 136, 748

Hart, J. D. 1997, Nonparametric Smoothing and Lack-of-Fit Tests (New York: Springer-Verlag)

Hirashita, H. 1999, ApJ, 510, L99

Hirashita, H., & Kamaya, H. 1999, AJ, submitted

Hoaglin, D. C., Mosteller, F., & Tukey, J. W. 1983, Understanding Robust and Exploratory Data Analysis (New York: John Wiley & Sons)

Ibata, R. A., Gilmore, G, & Irwin, M. J. 1994, Nature, 370, 194

Ikeuchi, S. 1988, Fundam. Cosmic Phys., 12, 255

Ikeuchi, S., & Tomita, H. 1983, PASJ, 35, 77

Ikuta, C., & Arimoto, N. 1999, PASJ, 51, 459

Kamaya, H., & Takeuchi, T. T. 1997, PASJ, 49, 271

Kennicutt, R. C., Jr. 1998, ApJ, 498, 541

Kennicutt, R. C., Jr., Tamblyn, P, & Congdon, C. W. 1994, ApJ, 435, 22

Lisenfeld, U., & Ferrara, A. 1998, ApJ, 496, 145

Lynden-Bell, D. 1975, Vistas in Astronomy, 19, 299

Maeder, A. 1992, A&A, 264, 105

Matteucci, F., & François, P. 1989, MNRAS, 239, 885

Nicolis, G., & Prigogine, I. 1977, Self-Organization in Nonequilibrium Systems (New York: Wiley and Sons)

Pagel, B. E. J. 1997, Nucleosynthesis and Chemical Evolution of Galaxies (Cambridge: Cambridge University Press)

Rao, C. R. 1973, Linear Statistical Inference and Its Applications, 2nd ed., John Wiley & Sons, New York

Rocha-Pinto, H. J., & Maciel, W. J. 1996, MNRAS, 279, 447

Rocha-Pinto, H. J., Scalo, J., Maciel, W. J., & Flynn, C. 2000a, ApJ, 531, L115 (R00)

Rocha-Pinto, H. J., Maciel, W. J., Scalo, J., & Flynn, C. 2000a, A&A, submitted (astro-ph/0001382)

Salpeter, E. E. 1955, ApJ, 121, 161

Schmidt, M. 1959, ApJ, 129, 243

Searle, L., & Zinn, R. 1978, ApJ, 225, 357

Soderblom, D. R., Duncan, D. R., & Johnson, D. R. H. 1991, ApJ, 375, 722

Sommer-Larsen, J. 1996, ApJ, 457, 118

Sommer-Larsen, J., & Antonuccio-Delogu, V. 1993, MNRAS, 262, 350

Tinsley, B. M. 1980, Fundam. Cosmic Phys., 5, 287

Tomita, A., Tomita, Y., & Saitō, M. 1996, PASJ, 48, 285

Twarog, B. A. 1980, ApJ, 242, 242

Wakker, B. P., & van Woerden, H. 1997, ARA&A, 35, 217

Whittet, D. C. B. 1992, Dust in the Galactic Environment (New York: IOP)

This preprint was prepared with the AAS LaTeX macros v5.0.

Table 1: Examined Parameters and ${\chi_0}^2$.

$\tau_{\rm sf}$[a]	$t_{\rm sf}$ (Gyr)	$\tau_{\rm in}$[b]	$t_{\rm in}$ (Gyr)	${\chi_0}^2$
0.4	6.0	1.5	23	172
0.7	11	0.8	12	172
1.0	15	0.6	9	172

[a]The gas consumption timescale ($t_{\rm sf}$) normalized by $T_{\rm G} = 15$ Gyr.

[b]The gas infall timescale ($t_{\rm in}$) normalized by $T_{\rm G} = 15$ Gyr.

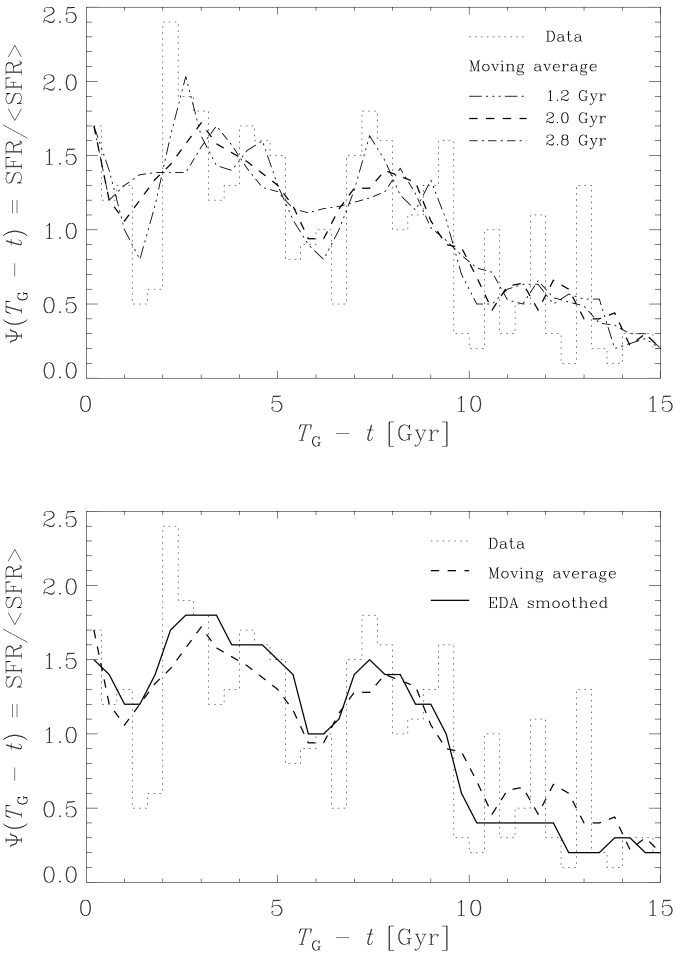

Fig. 1.— The smoothed star formation history of the Galaxy. In the upper panel, we show the smoothing result by moving average. The dot-dot-dot-dashed line is the smoothed SFR with smoothing kernel width of 1.2 Gyr, strong dashed line is the smoothed SFR with 2.0 Gyr kernel, and dot-dashed line is the smoothed SFR with 2.8 Gyr kernel. In the lower panel, the dashed line represents the moving average of 2.0 Gyr kernel, and the solid line is the smoothed SFH by the moving median method of the exploratory data analysis. We observe that the 1.2-Gyr kernel is not sufficient to smooth the varying SFH.

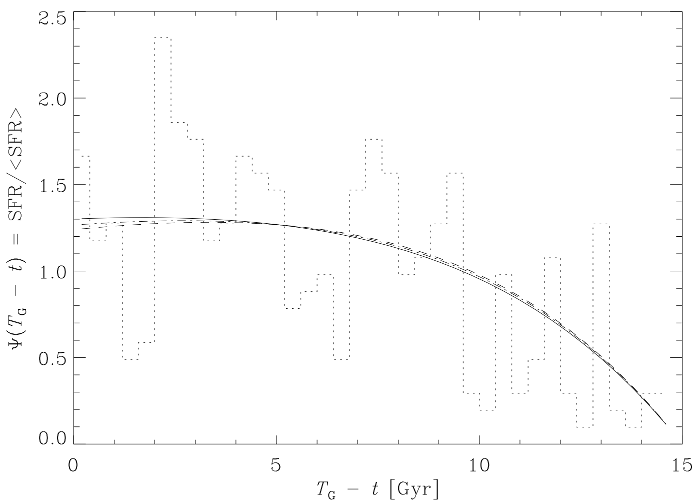

Fig. 2.— Star formation histories for the parameter sets in Table 1. The dotted line is the observed star formation history in R00. The solid, dashed, and dash-dotted lines present the cases of ($\tau_{\rm sf}$, $\tau_{\rm in}$) = (0.4, 1.5), (0.7, 0.8), and (1.0, 0.6), respectively, though it is difficult to distinguish the three lines.

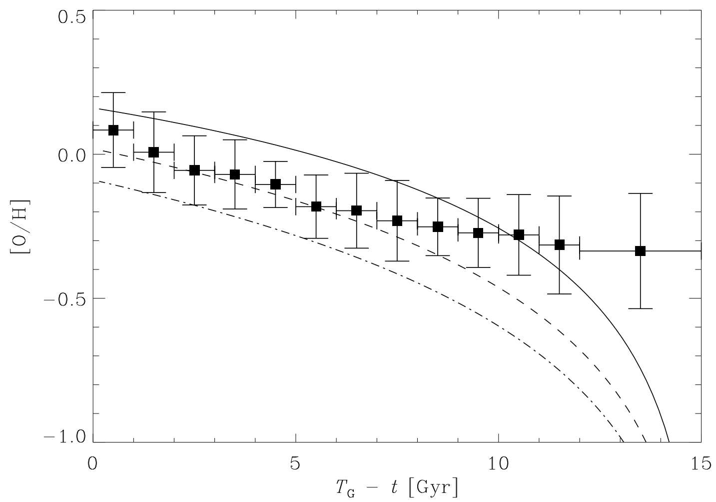

Fig. 3.— Time evolution of oxygen abundance $X_{\rm O}$ for the three sets of the parameters in Table 1. The solid, dashed, and dash-dotted lines present the cases of ($\tau_{\rm sf}$, $\tau_{\rm in}$) = (0.4, 1.5), (0.7, 0.8), and (1.0, 0.6), respectively. Contrary to Fig. 2, we can easily distinguish the three lines. The true parameter set seems to lie between ($\tau_{\rm sf}$, $\tau_{\rm in}$) = (0.4, 1.5) (the solid line) and ($\tau_{\rm sf}$, $\tau_{\rm in}$) = (0.7, 0.8) (the dashed line), though uncertainty and discrepancy exist.

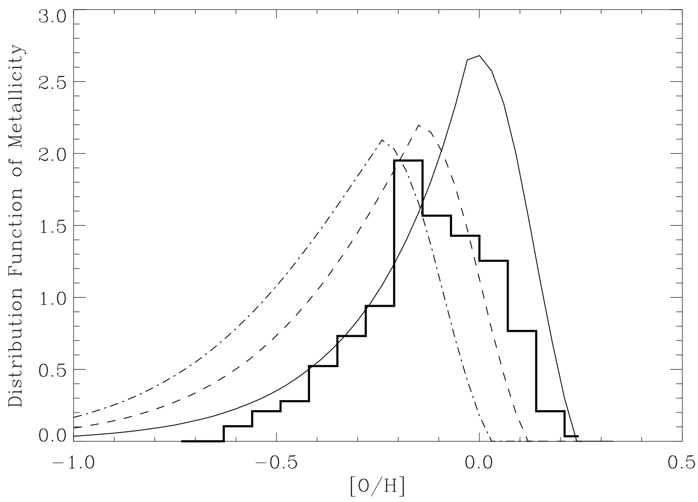

Fig. 4.— Distribution of the G-dwarf metallicity. for the three sets of the parameters in Table 1. The solid, dashed, and dash-dotted lines present the cases of $(\tau_{\rm sf},\, \tau_{\rm in}) = (0.4, 1.5), (0.7, 0.8)$, and $(1.0, 0.6)$, respectively. The histogram shows the data by Rocha-Pinto & Maciel (1996). Again the true parameter set seems to lie between $(\tau_{\rm sf},\, \tau_{\rm in}) = (0.4, 1.5)$ (the solid line) and $(\tau_{\rm sf},\, \tau_{\rm in}) = (0.7, 0.8)$ (the dashed line), though uncertainty and discrepancy exist.

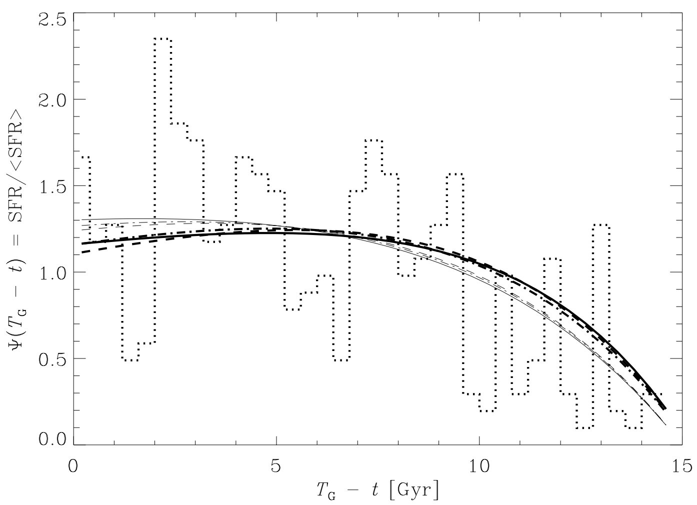

Fig. 5.— Star Formation History in the non-recycling model ($R = 0$) for the three parameters (*thick lines*) as an extreme case, where the timescale of the recycling is very large. The star formation history in the instantaneous recycling model is also shown (*thin lines*). The solid, dashed, and dash-dotted lines present the cases of $(\tau_{\rm sf},\, \tau_{\rm in}) = (0.4, 1.5), (0.7, 0.8)$, and $(1.0, 0.6)$, respectively.

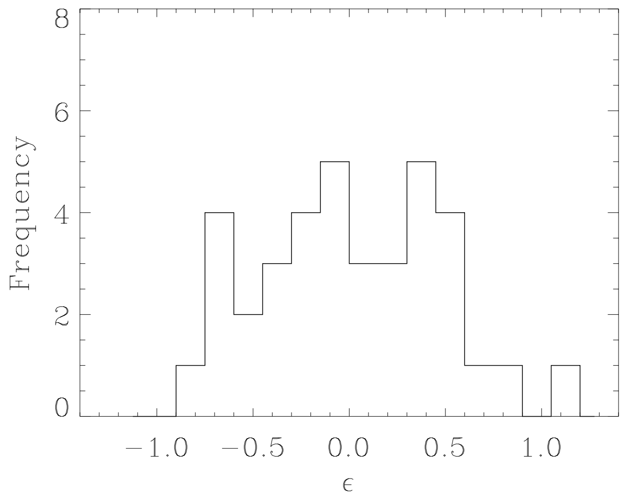

Fig. 6.— Distribution of the residual component of the star formation rate, ε.